

## Properties of liquid arsenic: A theoretical study

X.-P. Li\*

*Department of Physics, State University of New York at Stony Brook, Stony Brook, New York 11794-3800*

(Received 11 September 1989)

Various properties of liquid arsenic are calculated within the formalism of the quantum local-density-functional approximation, using the molecular-dynamics method proposed by Car and Parrinello. The structure of liquid arsenic is found to be similar to its ground-state, rhombohedral crystal structure, with coordination number 3 (in agreement with neutron-diffraction experiments), and has similar bond-angle, pyramid-height, and pyramid-angle distribution functions. Liquid arsenic is found to be a semiconductor with an energy gap of 0.15 eV. These results are consistent with the picture that the threefold coordination arises from a Peierls-type distortion from a sixfold-coordinated, simple-cubic-like structure. High-density and high-temperature properties are also studied, and it is shown that a crossover to a sixfold-coordinated metallic liquid will occur at high density, but not at high temperature. The structural properties of liquid arsenic are also studied by simulations employing pair potentials derived from second-order perturbation theory, which work surprisingly well, while showing small but significant differences from the *ab initio* simulations.

### I. INTRODUCTION

The recent neutron-scattering experiment of Bellissent *et al.*<sup>1</sup> showed that in contrast to the group-IV elemental semiconductors Si and Ge which, upon melting, increase their coordination number from 4 to more than 6 and undergo a semiconductor-to-metal phase transition, the coordination number of liquid arsenic remains the same as its crystal structures, and liquid arsenic is a narrow-band-gap semiconductor, while their crystal structures are either semimetal (rhombohedral, also called *A7*, the ground state) or semiconductor (orthorhombic).

An arsenic molecule in gas phase consists of a perfect tetrahedron of 4 atoms. Or if one face of the tetrahedron is put on a horizontal plane, it looks like a pyramid as shown in Fig. 1(a). The tetrahedron distorts in condensed phases into a flattened pyramid shape illustrated in Fig. 1(b), with the three bonds within the base face generally broken. The crystal and amorphous phases of arsenic can be viewed as different arrangements of the pyramids; their coordination number (3), bond lengths ( $\sim 2.5 \text{ \AA}$ ), and bond angles ( $\sim 97^\circ$ ) staying practically the same. The experiment of Bellissent *et al.*<sup>1</sup> indicates that the local structure of *liquid* arsenic is also similar. The variation in electronic behavior of different structures—ranging from semimetal to semiconductor—reflects the different arrangement of the pyramids that determines the overall density.<sup>2</sup>

With the help of first-principles, Hohenberg-Kohn-Sham-type local-density-functional<sup>3</sup> (LDA) calculations carried out by several groups,<sup>4-6</sup> a simple and elegant picture has emerged for an understanding of the crystal structures of arsenic. The valence-electronic configuration of an arsenic atom is  $4s^2 4p^3$ . The *s* level is far below the *p* level, and the fully occupied *s* band does not contribute much to the cohesion of the crystal. The *p*

level is half filled with three electrons. From the simple view of chemical bonds, the *p* bonds should be orthogonal to each other, which leads to an isotropic, sixfold-coordinated simple cubic (sc) or related structure, as shown in Fig. 2(a). However, such a structure is unstable against the doubling of the periodicity, or a three-dimensional analog of a Peierls distortion, for a half-filled band. One way the Peierls distortion works is to move one plane of atoms perpendicular to the threefold axis in sc in the direction of the threefold axis (similar to the one-dimensional dimerization), resulting in alternations of short covalent bonds and long, van der Waals-like bonds, as shown in Fig. 2(b): this is the *A7* structure. Now the coordination number becomes 3, the bond angle becomes a little bigger than  $90^\circ$ , and double layers form. The similar threefold coordinated, double-layer-like orthorhombic structure may be understood similarly. The electronic density of states (DOS) obtained by Mattheiss *et al.*<sup>6</sup> shows clearly how the Peierls distortion stabilizes the *A7* structure against the sc structure. The DOS of sc

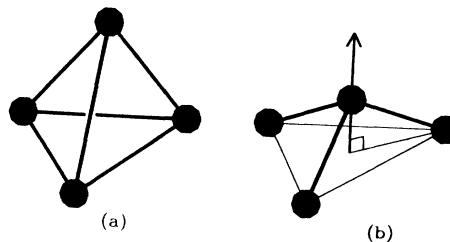


FIG. 1. Basic unit of atoms existing in various phases of arsenic. (a) A tetrahedron of 4 atoms existing as a molecule; (b) a pyramid or a flattened tetrahedron existing in condensed phases, the direction of which is represented by the arrow.

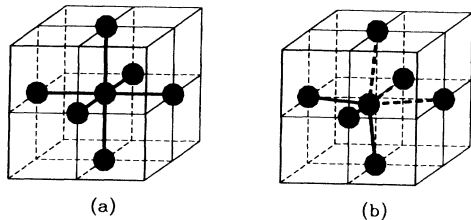


FIG. 2. Illustration of a three-dimensional Peierls distortion. (a)  $p$ -bonded simple-cubic structure; (b) rhombohedral structure resulted from a Peierls-distorted simple-cubic structure.

has the  $s$  peak well separated from the  $p$  peak as expected, and the Fermi energy is right in the middle of the  $p$  peak. Since the DOS at the Fermi surface is large, sc would be a good metal. Because of the Peierls distortion, each peak splits into two. The splitting of the  $p$  peak opens a deep minimum at the Fermi energy, moves some states just below the Fermi energy to lower energy and therefore lowers the total energy and stabilizes the  $A7$  structure against the sc structure, and causes the DOS reaching its minimum value at the Fermi energy and as a result makes the  $A7$  structure of arsenic a semimetal. The Peierls distortion argument gives all major features of the  $A7$  structure, and is well accepted.

Gaspard *et al.*<sup>7</sup> showed that a Peierls-type distortion does not necessarily require periodicity; Bellissent *et al.*<sup>1</sup> naturally suggested that the structure of liquid arsenic is also due to a Peierls-type distortion from a sixfold coordinated, sc like liquid. Since the Peierls distortion is non-perturbative and involves a complicated balance between the energies contributed from electrons and ions, we would expect that in order to understand the properties of liquid arsenic, the electrons must be treated in an exact and explicit way. But surprisingly, the molecular-dynamics simulations of Hafner<sup>8</sup> using pair potentials derived from second-order perturbation theory gave good pair-correlation function compared with experiment. This kind of potential is expected to work for near free-electron metals,<sup>9</sup> and indeed the second-order perturbation theory is not good enough to explain the  $A7$  crystal structure of arsenic.<sup>10</sup> It is encouraging that such a potential worked for liquid arsenic, which may be a small gap semiconductor.<sup>1</sup> Based on his simulations, Hafner argued that a Friedel modulation does an equally good job as a Peierls distortion does to explain the threefold coordination of liquid arsenic.

Early experiments<sup>11</sup> showed a phase transformation of crystal arsenic at high pressure. The linear augmented-plane-wave method (LAPW) calculation of Mattheiss *et al.*<sup>6</sup> suggested that this is an  $A7$  to sc structural transformation corresponding to the disappearance of the Peierls distortion, whereas the *ab initio* pseudopotential calculations of Needs *et al.*<sup>4</sup> suggested that an  $A7$  to sc transformation is unlikely to happen. What happens to liquid arsenic at high pressure and high temperature is also an interesting and important question.

We have carried out the first *ab initio* calculations for

liquid arsenic within LDA and using norm-conserving pseudopotentials.<sup>12</sup> Since such *ab initio* calculations are seriously limited by computer time and memory, simulations employing interatomic pair potentials derived from second-order perturbation theory are performed for comparison with the *ab initio* calculations. The major results have been reported earlier;<sup>13</sup> this paper provides additional results and details. The methods used will be described in Sec. II; properties of liquid arsenic near the triple point from the *ab initio* simulations and from the pair-potential simulations are reported in Secs. III and IV, respectively; high-density and high-temperature properties are predicted in Sec. V; and Sec. VI gives our conclusions.

## II. METHOD

The method we use to carry out this study is molecular-dynamics simulations, i.e., atoms are treated as classical particles and Newton's equations of motion are solved to generate atomic configurations. A faithful representation of the interaction between atoms is then crucial to the validity and accuracy of the simulations. We use two methods to represent the interactions; one is, suggested by Car and Parrinello (CP),<sup>14</sup> to treat electrons explicitly within LDA, and to calculate the forces according to Hellmann-Feynman theorem; the other is to include the role of electrons implicitly in an approximate pair potential.

### A. CP method

The total energy of a many-electron system within LDA is

$$E[\{\psi_i(\mathbf{r})\}, \{\mathbf{R}_I\}, \{\alpha_\nu\}] = \sum_i^{\text{occ}} f_i \left\langle \psi_i \left| \frac{\mathbf{p}^2}{2m} \right| \psi_i \right\rangle + U[n_e(\mathbf{r}), \{\mathbf{R}_I\}, \{\alpha_\nu\}], \quad (1)$$

where  $n_e(\mathbf{r})$  is the electron density,  $\{\psi_i(\mathbf{r})\}$  are the electron wave functions,  $\{\mathbf{R}_I\}$  are the positions of the ions, and  $\{\alpha_\nu\}$  are possible external variables. To find the ground state, CP suggested to minimize the total energy with respect to all possible degrees of freedom using simulated annealing or downhill-type minimization algorithms. The more important aspect of the CP method is that it can be used to calculate finite-temperature properties within Born-Oppenheimer (BO) approximation. Let the ions follow Newton's equations of motion, and so

$$M_I \ddot{\mathbf{R}}_I = - \frac{\partial E}{\partial \mathbf{R}_I}. \quad (2)$$

Strictly speaking, the energy  $E$  here is the electronic ground state given by

$$0 = - \frac{\delta E}{\delta \psi_i^*(\mathbf{r}, t)} + \sum_j \Lambda_{ij} \psi_j(\mathbf{r}, t), \quad (3)$$

where  $\Lambda_{ij}$  are Lagrange multipliers to enforce the orthonormal constraints. Instead, CP suggested association to each electronic degree of freedom a fictitious mass  $\mu$ , and let them also follow Newton's equations of motion so that

$$\mu \ddot{\psi}_i(\mathbf{r}, t) = -\frac{\delta E}{\delta \psi_i^*(\mathbf{r}, t)} + \sum_j \Lambda_{ij} \psi_j(\mathbf{r}, t). \quad (4)$$

Equation (4) is a good approximation of Eq. (3) if  $\mu$  is small compared with  $M_j$ . The electronic degrees of freedom can be allowed to gain only a little fictitious kinetic energy, corresponding to a small thickness of the BO surface. This method worked very well for semiconductors, and has been successfully used to a variety of *s-p*-bonded systems, including selenium and sulphur clusters by Hohl *et al.*,<sup>15</sup> amorphous silicon by Car and Parrinello,<sup>16</sup> silicon microclusters by Ballone *et al.*,<sup>17</sup> and amorphous carbon by Galli *et al.*<sup>18</sup> Recently, this method is believed to work also for metals after some modifications,<sup>19,20</sup> and has been successfully applied to liquid silicon by Štich *et al.*,<sup>21</sup> to liquid gallium arsenide by Zhang *et al.*,<sup>22</sup> to liquid carbon by Galli *et al.*,<sup>23</sup> and to liquid sodium by Qian *et al.*<sup>24</sup>

### B. Pair potential

Recently a lot of empirical potentials have appeared in the literature mainly for group-IV elements Si or C, and a lot of interesting work has been done using these potentials.<sup>25</sup> But here we choose to use the pair potential derived by treating the valence electrons as a homogeneous electron gas and the positively charged ions as perturbations to second order. This method is more systematic, but the potentials fail to give stable covalent structures. The derivation of the pair potentials can be found in Ref. 26. The result is very simple and physical: the pair potential is the sum of the direct Coulomb repulsion between two ions, and the attraction of the first ion to the screening charge distribution induced by the second ion:

$$\Phi(k) = \frac{4\pi Z^2 e^2}{k^2} + v_{ps}(k) \chi(k) v_{ps}^{scr}(k), \quad (5)$$

where  $\chi$  is the linear-response function of the interacting electron gas,  $v_{ps}$  the bare pseudopotential between a valence electron and an ion, and  $v_{ps}^{scr}$  the screened pseudopotential.

Hafner and Heine<sup>27</sup> used such pair potentials to explain crystal structures of elemental metals and Hafner and Kahl<sup>28</sup> to explain liquid structures. Recently, Hafner<sup>8</sup> employed such a pair potential to study liquid arsenic and obtained good results. Following Hafner, we use the Ichimaru-Utsumi<sup>29</sup> dielectric function and Ashcroft empty core pseudopotential.<sup>30</sup> The pair potentials for arsenic at two different densities are shown in Fig. 3. They are used in this study.  $R_{core}$ , the core radius of Ashcroft pseudopotential, is 0.53 Å.

## III. LIQUID ARSENIC: *ab initio* SIMULATIONS

### A. Computational details

We employ the CP method within LDA and with use of norm-conserving pseudopotentials. Only the *s* nonlocality is included with the pseudopotential of *p* state treated as the local part. Kleinman and Bylander's factorized form<sup>31</sup> of the nonlocal pseudopotential is used to

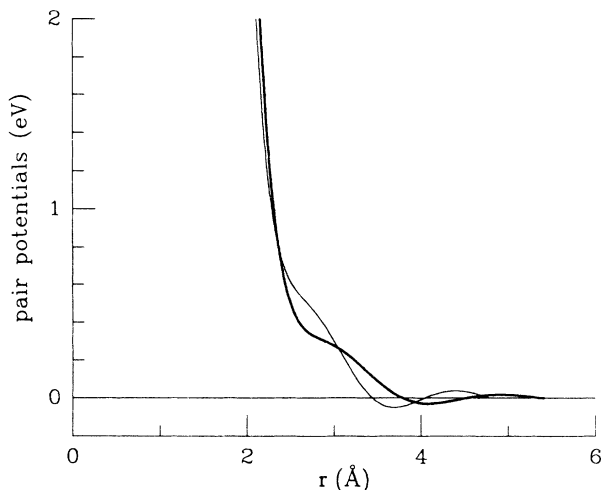


FIG. 3. Pair potentials from second-order perturbation theory for arsenic at two different densities. The thick line is at  $n=0.04220$  atoms/Å<sup>3</sup>, and the thin line is at  $n=0.06297$  atoms/Å<sup>3</sup>.

speed the calculations. Liquid arsenic is simulated by 64 atoms in a cubic supercell with periodic boundary conditions. This size is about the limit that we can handle with the present supercomputers, and is large enough to give good ensemble averages as we will show by analysis of size dependence of pair potential simulations, where much larger sizes are feasible. The fictitious mass of the electrons is 400 times the true electron mass, which is still much smaller than the ion mass of arsenic. The time step is 3 a.u., or  $7.26 \times 10^{-17}$  sec. To give an idea how large this time step is, an As<sub>2</sub> molecule vibrates a period in about 800 time steps.

The size of the unit cell,  $22.2826a_B$ , is chosen so that the density is 4.856 g/cm<sup>3</sup>, which is given and used by Bellissent,<sup>32</sup> who took it from the early experiment of Klemm *et al.*<sup>33</sup> Another experiment<sup>34</sup> showed that at the triple point, the density of liquid arsenic is 5.22 g/cm<sup>3</sup>. The difference reflects the experimental uncertainty, and does not affect our results and conclusions.

A very important parameter is the energy cutoff of the plane-wave basis set. A test calculation shows that a 16 Ry energy cutoff is good enough to describe an As<sub>2</sub> molecule. We performed a simulation of liquid arsenic with an energy cutoff of 6 Ry,<sup>35</sup> hoping that although it is lower than needed for an As<sub>2</sub> molecule, it may be adequate for the liquid, where atoms are more uniformly distributed and wave functions are expected to be more smooth. But the results are not satisfactory. The first peak in the pair-correlation function is too high, the peak positions are too small, and the coordination number is too small compared with experiment, showing that 6 Ry energy cutoff is also not large enough for liquid arsenic. For all the calculations reported here, an energy cutoff of 12 Ry is used, which was also used by Needs *et al.*<sup>4</sup> to calculate the properties of crystalline arsenic. Only one  $\mathbf{k}$  point, the  $\Gamma$  point, is used to calculate the self-consistent electron density and the DOS, and the fact that all the

wave functions in coordinate space are real at the  $\Gamma$  point is used.

Initially atoms are randomly displaced from a simple-cubic crystal structure, then relaxed and temperature raised to more than 6000 K to ensure a molten system, then lowered gradually to about 1150 K, close to the triple-point temperature 1090 K. Because of the small size of the system and therefore the large fluctuation, temperature is determined to only  $\pm 100$  K. After equilibration, statistics are collected in 4000 time steps.

### B. Structural properties

The first quantity we can calculate from a successive sequence of coordinates is the mean-square displacement as a function of time interval, shown in Fig. 4. The behavior is typical. In a small time interval ( $t < 10^{-13}$  sec), the curve is parabolic and the motion of the atoms are mainly ballistic like, or strongly correlated to their motion a time  $t$  before. After about  $2 \times 10^{-13}$  sec, the curve falls approximately onto a straight line (this time interval is also typical. For liquid water at room temperature,<sup>36</sup> for example, the diffusion coefficient  $D = 2.85 \times 10^{-5}$  cm<sup>2</sup>/sec is in the same order of magnitude as that of liquid arsenic from our estimate, and the mean-square displacement also falls approximately onto a straight line after about  $2 \times 10^{-13}$  sec.) indicating that our molecular dynamics run is long enough to reach the uncorrelated region and to cover enough phase space to give reliable ensemble averages. From the slope of the fitted straight line, we estimate the self-diffusion coefficient  $D$  to be  $6.0 \times 10^{-5}$  cm<sup>2</sup>/sec; we are not aware of an experimental result to compare with.

Figure 5(a) shows the pair-correlation function from our *ab initio* simulations and from Hafner's.<sup>8</sup> They are qualitatively similar. The coordination number defined as the number of nearest neighbors is generally calculated

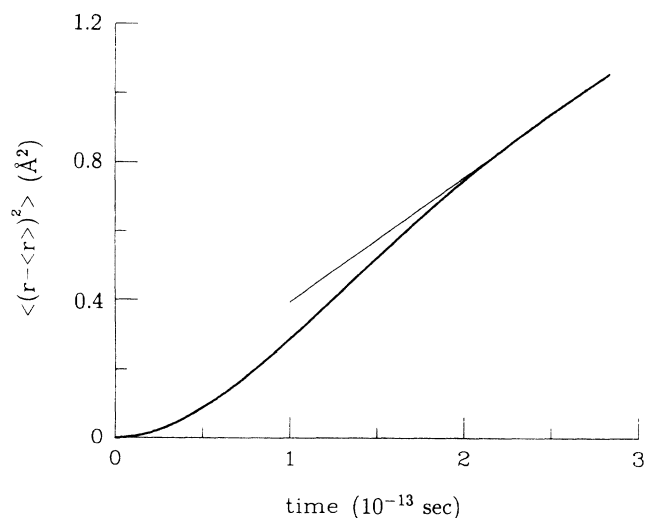


FIG. 4. Mean-square displacement of arsenic atoms in the near triple-point liquid state as a function of time from CP method. The straight line is a least-squares fit.

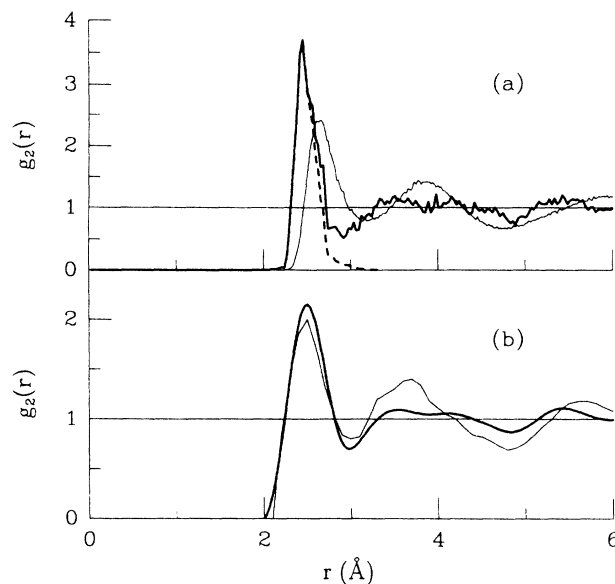


FIG. 5. The pair-correlation function  $g_2(r)$  vs separation  $r$  for liquid arsenic near the triple point. (a) The thick line is from the *ab initio* simulations, the dashed line is the  $g_2(r)$  for only the three nearest-neighbor atoms (see text), and the thin line is from Ref. 8. (b) The thick line is the  $g_2(r)$  from the present work broadened by the experimental  $q_{\max}$  and the thin line is the experimental result from Ref. 1.

according to the formula

$$Z = 4\pi\rho \int_0^{R_c} dr r^2 g_2(r), \quad (6)$$

where  $\rho$  is the average number density and  $R_c$  is a cutoff distance, usually taken as the position of the first minimum in  $g_2(r)$ . But since the second peak is much broader than the first peak,  $Z$  so defined (let us call it the number of atoms under the first peak) may include some contributions from the second peak. To avoid ambiguity and to find the coordination number in a straightforward way, we show, in dashed line in Fig. 5(a), the pair-correlation function for the three nearest neighbors of each atom. It is almost in perfect coincidence with the first peak in  $g_2(r)$ , showing that the true coordination number is indeed 3. The differences on the right-hand side of the peak and the tail near 3  $\text{\AA}$  indicate the existence of some fourfold and twofold coordinated atoms. It is interesting to notice that at 2.7  $\text{\AA}$ , there is a sudden drop in  $g_2(r)$ . If we take the position of this sudden drop to be  $R_c$ , then we get  $Z = 3$  from Eq. (6), and the possibilities for an atom to be onefold through fivefold coordinated are 2.7%, 19.5%, 55.3%, 22.0%, and 0.4%, respectively, showing dominant threefold coordination. Hafner's result is qualitatively very similar to ours, but the first peak in his  $g_2(r)$  is much lower and broader, and he compared his  $g_2(r)$  directly with the experimental result of Bellissent *et al.*<sup>1</sup> Etherington *et al.*<sup>37</sup> argued that this kind of comparison is not very valid, because the experimental pair-correlation function was obtained with a

finite momentum range  $q_{\max}$  and is therefore not exact, whereas the pair-correlation function from simulations is “exact” in the sense that it is calculated in the coordinate space and no momentum cutoff is imposed. Bellissent *et al.*<sup>1</sup> observed this effect, and stated that if  $q_{\max}$  is increased, the height of the first peak in  $g_2(r)$  increases drastically to about 4. Our  $g_2(r)$  happens to show a peak height of about 4, and this may not be an accident. In order to do a valid comparison with experiment, our  $g_2(r)$  is broadened<sup>37</sup> with  $q_{\max} = 13 \text{ \AA}^{-1}$  and shown in Fig. 5(b) together with the experimental result. Over all, the agreement is fairly good. The positions of the first peak and the first minimum agree, and the structures of the second peak are qualitatively correct. Considering that there are no adjustable parameters in our simulations, this agreement is impressive. But the height of the second peak, the depth of the second minimum, and the position of the third peak are not quite right.

The static structure factor  $S(q)$  is defined by

$$S(q) = \frac{1}{N_a} \left\langle \sum_{ij} \exp[iq \cdot (r_i - r_j)] \right\rangle - N_a \delta_{q0}, \quad (7)$$

where  $N_a$  is the number of atoms in the system. Because of the small size of the system,  $S(q)$  so calculated fluctuates a lot and the fluctuations have to be removed by a suitable averaging scheme. Here we Fourier transform  $g_2(r)$  to obtain  $S(q)$  to check the peak positions [ $S(q)$  such obtained gives broader peaks, especially the first few of them, because of the  $r$ -range cutoff, but the peak positions are roughly correct<sup>37</sup>]. The result is shown in Fig. 6(a) as well as the experimental result. The overall agreement is again good, but the first two peaks are lower and broader than those of experiment, just the opposite as in  $g_2(r)$ , and can be understood similarly. The experimental  $S(q)$  is exact in principle, but the  $S(q)$  from simulations is not because the  $r$  range is limited to about 6 Å by the size of the system. In our result,  $S(q)$  has peaks at 2.85, 3.55, 5.70, 8.25, and 10.60 Å<sup>-1</sup>, in fairly good agreement with the experimental peak positions 2.45, 3.74, 5.86, 8.00, and 10.75 Å<sup>-1</sup>. Figure 6(b) reproduces Hafner’s result. Since the size in his simulations is large enough to distinguish small  $q$  differences, Hafner got the first two major peaks correctly separated from each other. But beyond the second peak, our *ab initio* results show slightly better agreement with experiment, especially the peak positions.

One of the advantages of computer simulations is that some quantities that are not easy to measure experimentally can be calculated easily. The bond-angle distribution function  $g_3(\theta)$  is one of such quantities that can help us gain more insight into the structure of a liquid.  $g_3(\theta)$  is defined as the possibility of finding an angle  $\theta$  between triplets of atoms, the bond length of which about the included angle are both less than the position of the first minimum in  $g_2(r)$ . The angle distribution function as a function of  $\theta$  is shown in Fig. 7(a). It is more natural to show it as a function of  $\cos\theta$ , since the solid angle increment is a constant for constant  $d \cos\theta$  but varies for constant  $d\theta$ . The fact that  $g_3(\theta)$  tends to zero at  $\theta = 180^\circ$  in Fig. 7(a) does not imply that the possibility of finding an

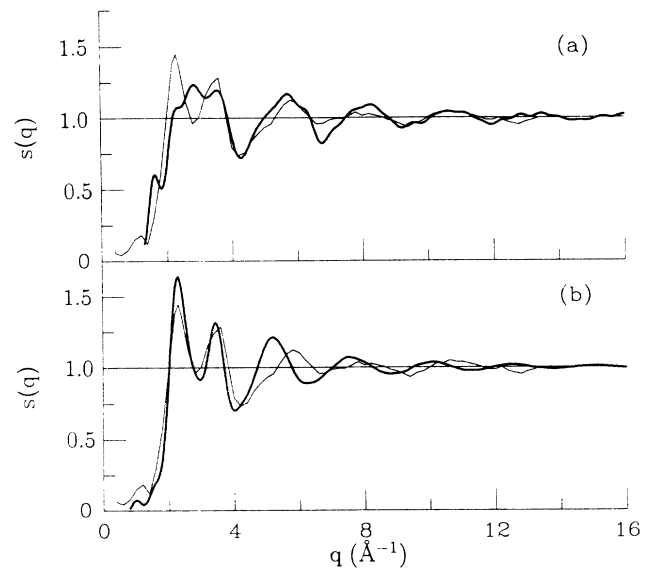


FIG. 6. Static structure factor  $S(q)$  for liquid arsenic near the triple point from (a) our *ab initio* simulations (thick line) and (b) Hafner’s pair-potential simulations (thick line). The thin lines are from experiment.

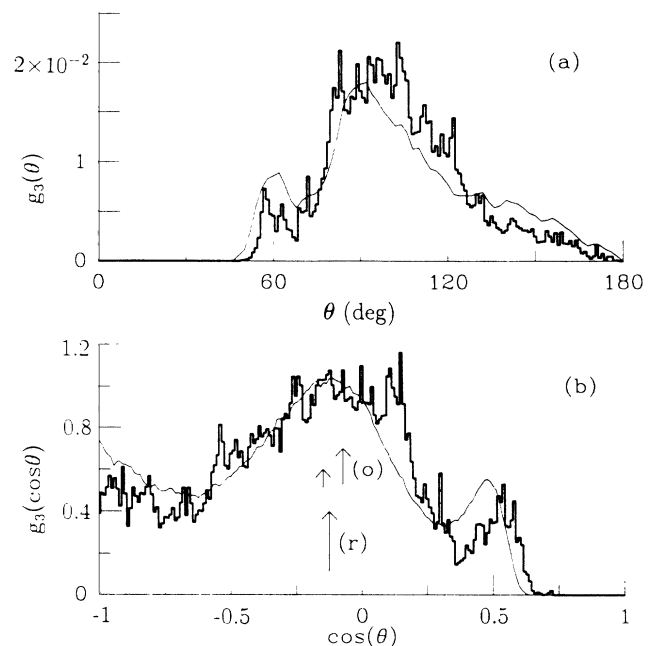


FIG. 7. Bond-angle distribution function  $g_3$  for liquid arsenic near the triple point. (a)  $g_3$  as a function of  $\theta$ . The histogram is from the present *ab initio* simulations and the thin line from Hafner’s pair-potential simulations. (b)  $g_3$  as a function of  $\cos\theta$ . The histogram is from the *ab initio* simulations and the thin line from our pair potential simulations, which should be the same as Hafner’s result. The arrows show the positions of the bond angle in rhombohedral ( $r$ ) and orthorhombic ( $o$ ) crystal structures with the lengths of the arrows representing the relative weight.

angle of  $180^\circ$  is zero, but rather the possibility is normalized to  $\sin\theta$ . Since Hafner plotted his bond-angle distribution function as a function of  $\theta$ , we plot it the same way for a convenient comparison. The two results are again very similar to each other, except that the peak around  $100^\circ$  in our result has more weight than Hafner's, and the subsidiary maximum at  $60^\circ$  is smaller. The bond angles are mainly distributed between  $80^\circ$  and  $125^\circ$ . The bond-angle distribution function *versus*  $\cos\theta$  is plotted in Fig. 7(b) [also shows the  $g_3(\cos\theta)$  from our Hafner-type pair potential simulations for comparison], showing that near  $\cos\theta = -1$  or  $\theta = 180^\circ$ , the possibility is nonzero, which is consistent with our naive expectation. The strong repulsive forces between atoms at short distance do not allow the bond angle to be close to zero, but nothing prevents it, and nothing enhances it also, to be close to  $180^\circ$  in a liquid; both calculations give  $g_3(\cos\theta = -1) \sim 0.5$ , which is the value that would be found if all angles were equally probable. The subsidiary maximum near  $\theta = 60^\circ$  ( $\cos\theta = 0.5$ ) indicates the existence of some equilateral triangles. Hafner concluded that the equilateral triangles are related to the "defects" (relative to an ideal continuous network with nearly ideal rhombohedral bond angles) in liquid arsenic, and such defects are tetrahedral groupings of four arsenic atoms just as they exist in gaseous arsenic. Although this conclusion is reasonable from this single piece of information, it is not the case from our *ab initio* simulations as we will show later.

An important feature of threefold coordination is that an atom and its three nearest-neighbor atoms form a pyramid as shown in Fig. 1(b). It is interesting to see what the pyramids look like in liquid arsenic. Since  $g_2(r)$  and  $g_3(\cos\theta)$  do not depend on the shape of pyramids very sensitively, we show, in Fig. 8  $g_4(r)$ , the distribution of the height of the pyramids, or the distance between an atom and the plane defined by its three nearest neighbors

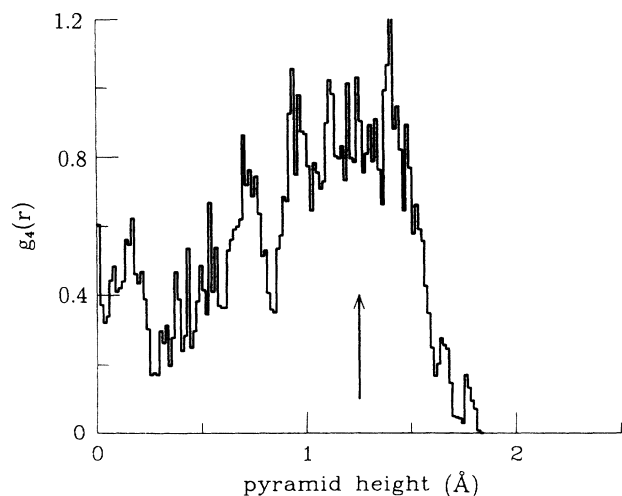


FIG. 8. Distribution function  $g_4(r)$  of the pyramid height for liquid arsenic near the triple point from *ab initio* simulations. The arrow shows the value for crystalline structures (both rhombohedral and orthorhombic) of arsenic.

[see Fig. 1(b)].  $g_4(r)$  shows a broad peak around  $1.25 \text{ \AA}$ , the value for crystal structures, indicating that the shape of the pyramids in liquid arsenic is very similar to that of the crystals. From the information given by  $g_2(r)$ ,  $g_3(\cos\theta)$ , and  $g_4(r)$ , we conclude that the local structure of liquid arsenic generated from *ab initio* simulations is similar to the crystal structures.

The two well-known crystal forms of arsenic have very similar local structures. It is natural to ask whether the short-range order of liquid arsenic is more similar to the rhombohedral or to the orthorhombic structure. This question cannot be answered by considering only  $g_2(r)$ ,  $g_3(\cos\theta)$ , and  $g_4(r)$  because there is almost no difference between the two structures as far as the nearest neighbors are concerned. In Fig. 7(b), the arrows show the positions of the bond angles in rhombohedral (*r*) and orthorhombic (*o*) crystal structures with the length of the arrows representing the relative weight. They are so close to each other that they can not be distinguished from each other in the liquid. Figure 1(b) defines the direction of a pyramid to be perpendicular to the base face and pointing from the base face to the apex atom. Since a widely accepted name for the angle between two bonds is "bond angle," we shall similarly call the angle between the directions of two neighboring pyramids "pyramid angle," which is helpful to distinguish the two crystal forms. To visualize the concept of pyramid angle, the inset of Fig. 9 gives directions of two neighboring pyramids that generally involves six atoms, but sometimes involves only five, or even four atoms as in a perfect, isolated tetrahedron of  $\text{As}_4$  molecule. The pyramid angles are always  $180^\circ$  in the rhombohedral structure, whereas in the orthorhombic structure,  $\frac{1}{3}$  of the pyramid angles are  $180^\circ$  and  $\frac{2}{3}$  are around  $48^\circ$ . The arrows below the histogram in Fig. 9 indicate the positions and relative weights of these angles, and the histogram shows the pyramid angle distribution function,  $g_6(\cos\theta)$ , of liquid arsenic from our *ab*

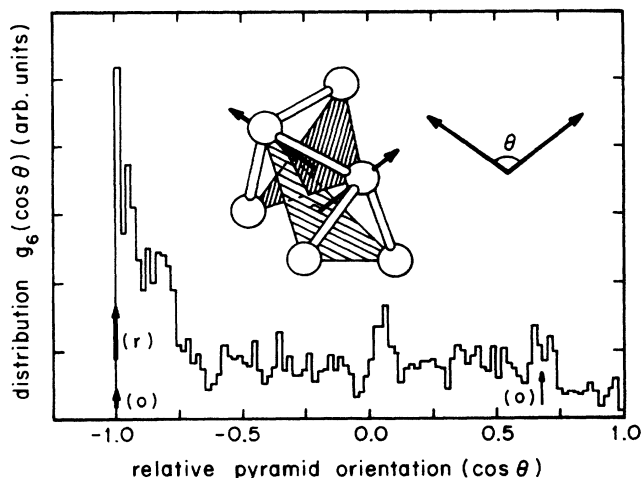


FIG. 9. Distribution function  $g_6(\cos\theta)$  of the angle between neighboring pyramid vectors for liquid arsenic near the triple point from the *ab initio* simulations. The inset illustrates the pyramid angle between two neighboring pyramids.

*initio* simulations. If the pyramids were completely randomly arranged, that is there were no correlation at all between neighboring pyramids, then  $g_6(\cos\theta)$  would be a constant except the smaller possibility near zero degree ( $\cos\theta=1$ ) because of topological reasons. This is almost true except the big peak around  $\cos\theta=-1$  ( $\theta=180^\circ$ ). This peak is so high that we have to believe that the neighboring pyramids are happy to sit in the opposite direction. Since only a very weak feature appears near  $\cos\theta \simeq 0.67$  ( $\theta \simeq 48^\circ$ )—one of the two pyramid angles in the orthorhombic structure, the pyramid angle distribution function is an evidence that the structure of liquid arsenic is more similar to the rhombohedral than to the orthorhombic structure.

If some moleculelike tetrahedrons existed, we would expect a peak near  $\theta=109^\circ$  or  $\cos\theta=-\frac{1}{3}$ . A very small peak around  $87^\circ$  appears instead. Therefore, perfect tetrahedrons similar to  $\text{As}_4$  molecules can be excluded; the defects Hafner suggested according to his  $g_3(\theta)$  do not exist in our liquid arsenic generated from *ab initio* simulations.

### C. Electronic and optical properties

In the CP method, the self-consistent electron densities are generated from the same procedure that derives the atomic configurations. These electron densities completely determine the electronic and related properties of the system according to density functional theory.

The electronic DOS of liquid arsenic is obtained by averaging over 40 configurations and is shown in Fig. 10. Also shown by a thin line is the DOS of the rhombohedral crystal structure calculated by Mattheiss *et al.*<sup>6</sup> They are very similar to each other. In both DOS's, the *s* and *p* states are separated by a deep minimum around  $-7$  eV, with the whole *s* peak far below the Fermi energy—consistent with the expectation that the *s* level

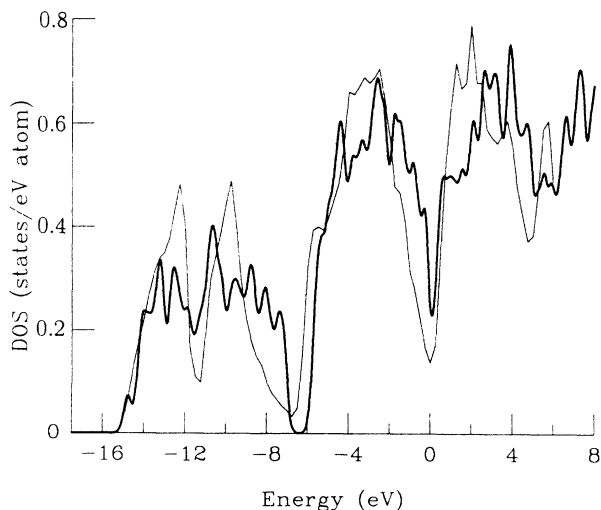


FIG. 10. Electronic DOS for liquid arsenic near the triple point from the present *ab initio* simulations (thick line) and for the rhombohedral-crystal structure from Ref. 6 (thin line).

has little contribution to the cohesion of the bulk arsenic. In the crystal, the *s* peak is split by a minimum at  $-12$  eV, and in both liquid and crystal there is a deep minimum at the Fermi energy splitting the *p* peak. This similarity suggests that (a) the local structure of liquid arsenic is indeed similar to the rhombohedral crystal structure, consistent with our previous finding; (b) since the Peierls distortion picture is so successful in explaining the rhombohedral structure, and since a Peierls distortion is so natural to understand the minima that split the *s* and *p* peaks, we have to conclude that it is still the Peierls distortion that is responsible for the liquid structure. The “Peierls gap,” i.e., the minimum at the Fermi energy, lowers the total energy and stabilizes the liquid structure against a sixfold coordinated liquid.

It is interesting to examine the possible localization of electronic states in a disordered system by the participation ratio defined as

$$L_i = \left[ \Omega \int d\mathbf{r} |\psi_i(\mathbf{r})|^4 \right]^{-1}, \quad (8)$$

where  $\psi_i(\mathbf{r})$  is the normalized wave function of the *i*th state and  $\Omega$  is the volume of the system. For a free particle state, i.e.,  $\psi(\mathbf{r})$  is a plane wave that is the most extended state, the participation ratio *L* is exactly 1. If a state only occupies a volume  $v < \Omega$ , then *L* is approximately  $v/\Omega$ . For an extended state *v*, though possibly small compared with  $\Omega$ , is proportional to  $\Omega$ ; but for a localized state, *v* is a constant regardless of  $\Omega$ . Therefore, for an infinitely large system, *L* is zero or finite for a localized or an extended state, respectively. But for a finite system as in our calculations, localized and extended states can not be distinguished strictly. Nevertheless, we can get at least a rough idea.

The participation ratio *versus* energy for liquid arsenic is shown in Fig. 11. It is interesting to notice that it has a steplike behavior. Comparing the energy axis with that

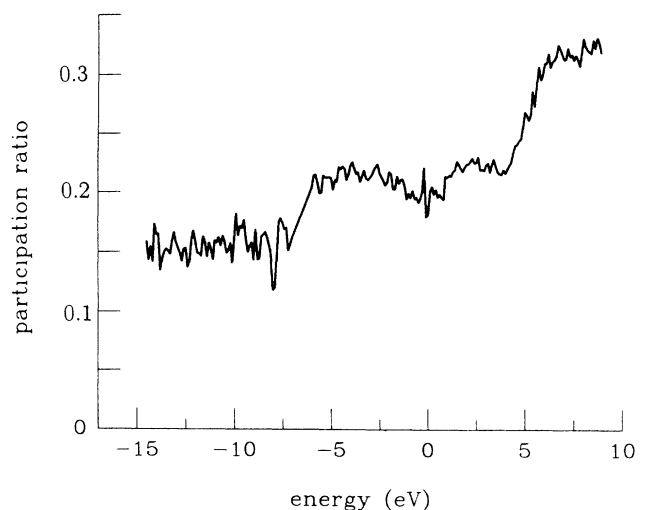


FIG. 11. Participation ratio vs energy from *ab initio* simulations for liquid arsenic near the triple point.

of the DOS, we observe that the participation ratio is approximately a constant for all the states that have the same symmetry (referring to angular momentum). This observation can be understood if wave functions in the liquid still retain some characteristics of wave functions in an atom in the radial direction as well as in the angular direction. No state has a particularly small participation ratio, indicating that there is no localized state, at least within the limitations of a 64 atom cell.

The imaginary part of the dielectric constant  $\epsilon_2(\omega)$ , which measures the light absorption, is calculated according to the Kramers-Heisenberg formula<sup>38</sup>

$$\epsilon_2(\omega) = \frac{8\pi^2 e^2}{\Omega m^2 \omega^2} \sum_i^{\text{occ}} \sum_j^{\text{unocc}} |\langle i | p_x | j \rangle|^2 \delta(\epsilon_j - \epsilon_i - \hbar\omega). \quad (9)$$

This formula (also called the Kubo-Greenwood formula) has been used by Allen and Broughton<sup>39</sup> to calculate the electrical conductivity of liquid silicon and a related formula was used by Allen and Feldman<sup>40</sup> to calculate the heat conductivity of amorphous silicon, and they are successful. In our calculations, this formula needs to be modified because the nonlocal pseudopotential does not commute with coordinate  $r$ .<sup>41,42</sup> But since the nonlocal pseudopotential is only a very small part of the potential, the correction is expected to be small. Therefore, we use the Kramers-Heisenberg formula as it is to calculate  $\epsilon_2(\omega)$ , and show the result in Fig. 12. An energy gap of 0.15 eV appears. In fact, an energy gap opens at the Fermi energy of the DOS for each configuration and the smallest one is 0.15 eV. But the averaged DOS shows a minimum instead of a gap because of the small size of the system and, therefore, the relatively large fluctuations of the Fermi energy. In a finite system, a very small gap is generally not reliable because the energy spectrum is quasicontinuous. Here we tend to believe that this gap is large enough to be true because the average level spacing is less than 0.05 eV and LDA generally underestimates gaps of semiconductors (a comparison of Fig. 12 with

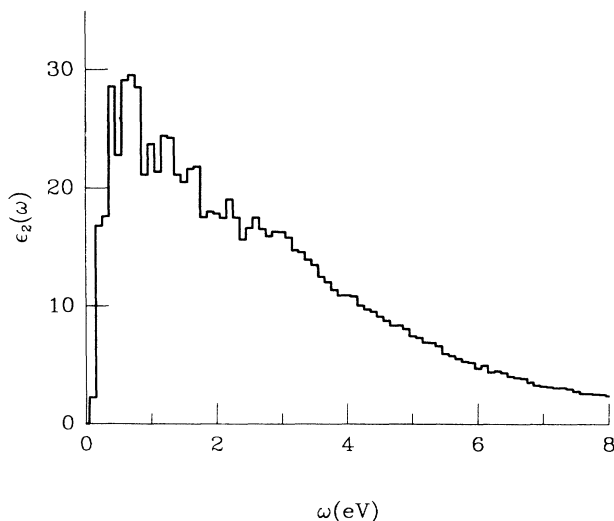


FIG. 12. Imaginary part of the dielectric constant vs energy from *ab initio* simulations for liquid arsenic near the triple point.

Fig. 21, which shows metallic behavior is also helpful), but it is smaller than the quoted experimental result,<sup>1</sup>  $\sim 0.5$  eV. The dc dielectric constant  $\epsilon_1(0)$  is estimated to be 48.7 according to

$$\epsilon_1(0) - 1 = \frac{1}{\pi} \int_{-\infty}^{\infty} \frac{1}{\omega} \epsilon_2(\omega) d\omega. \quad (10)$$

Unfortunately, we are not aware of any experimental measurements of light absorption for liquid arsenic.

#### IV. LIQUID ARSENIC: PAIR-POTENTIAL SIMULATIONS

First of all, Hafner's static structure factor  $S(q)$ , pair-correlation function  $g_2(r)$ , and bond-angle distribution function  $g_3(\theta)$  are exactly reproduced using the pair potential shown by the thick line in Fig. 3 (which is exactly the same as the one Hafner used) with a cutoff radius of 10 Å, and using 500 atoms in a cubic supercell with periodic boundary conditions (Hafner used cutoff radius of about 10 Å also and 864 atoms).

Hafner argued that the threefold coordination in liquid arsenic is due to a Friedel modulation. As shown in Fig. 3, the pair potential has an inflection point near 3 Å, which is a result of the Friedel oscillations extended to short range. The simple pair potential prefers a close-packed-type structure; the fixed density forces the nearest-neighbor distance to be around 3 Å; and the inflection point splits the close-packed nearest neighbors into two shells with the first shell containing about 3 atoms. In order to see the effects of the intermediate- and long-range part of the Friedel oscillations, we cut the potential off at about 5.7 Å, i.e., only retaining one oscillation. The pair-correlation functions and bond-angle distribution functions are shown in Figs. 13 and 14, together with the results using the cutoff radius 10 Å. The differences are almost invisible. We agree with Hafner that the approximate threefold coordination is because of the inflection point near 3 Å in the pair potential, and the inflection is a result of the Friedel oscillation. But the intermediate- and long-range part of the Friedel oscillations are not important at all.

One question frequently raised about the *ab initio* simulations is how reliable it is using a system of 64 atoms to represent the liquid bulk. The *ab initio* simulation itself can not clarify this because calculations with larger systems are impossible. Clearly this is a place where pair-potential simulations can help. The results of pair-potential simulations with 64 atoms (cutoff radius for the pair potential is 5.7 Å) are also shown in Figs. 13 and 14. The differences are again invisible except the worse statistics. Therefore, 64 atoms are enough to give good ensemble averages and to properly describe the properties of a liquid in the short range.

Although our pair-correlation function is identical to Hafner's, we analyze it in a different way. Hafner fitted the peaks with Gaussians to find the coordination number, which we think is somewhat arbitrary. In Fig. 15(a) in the dashed line, we plot the  $g_2(r)$  for only the three



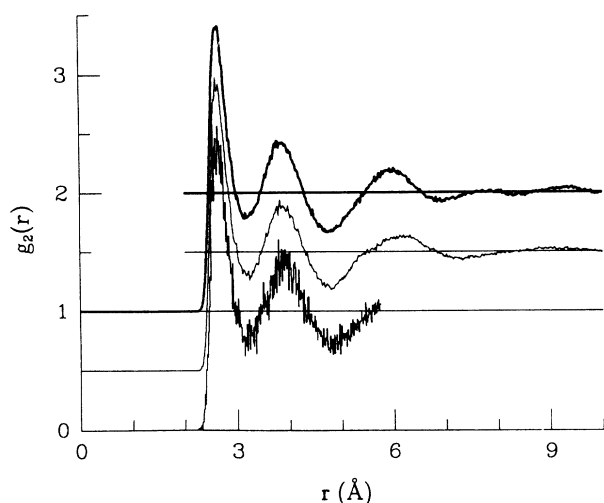


FIG. 13. Pair-correlation functions from various pair-potential simulations at low density. Thick line: 500 atoms (shifted up by 1.0 for clarity), pair potential is cutoff at  $R_c = 10$  Å; thin line: 500 atoms (shifted up by 0.5),  $R_c = 5.7$  Å; histogram: 64 atoms,  $R_c = 5.7$  Å.

nearest-neighbor atoms. It is clearly different from the first peak in  $g_2(r)$ . Therefore, the coordination number cannot be identified as 3 from our criterion. The solid thin line, the  $g_2(r)$  from the four nearest-neighbor atoms, is in better coincidence with the first peak in  $g_2(r)$ , indicating that the coordination number is 4. Therefore, the coordination number from pair-potential simulations is different from that of *ab initio* simulations. As discussed in Sec. III C, the calculated  $g_2(r)$  has to be broadened to do a valid comparison with experiment. The broadened  $g_2(r)$  is shown in Fig. 15(b) as well as the experimental result. Overall agreement with experiment is about the same as in the *ab initio* case [Fig. 5(b)], being worse at small  $r$  and better at larger  $r$ .

The number of atoms under the first peak in  $g_2(r)$  is defined in Eq. (6) with  $R_c$  the position of the first minimum that is different from the coordination number

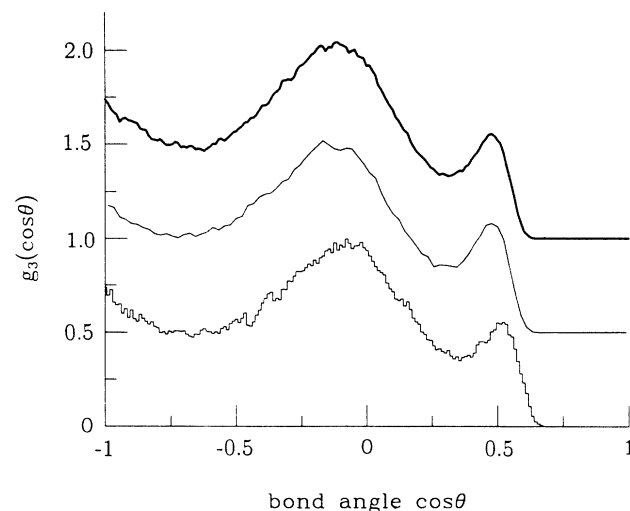


FIG. 14. Bond-angle distribution functions from various pair-potential simulations at low density. The line convention is the same as in Fig. 13.

because no correction from the second peak is made; and the number of atoms under the second peak is defined in the same way except that the integral is from the first minimum to the second minimum, and so on. We find that the number of atoms under the first peak of  $g_2(r)$  are 3.9, 3.82, and 4.48 from experiment, *ab initio* and pair-potential simulations, respectively, as listed in Table I. The *ab initio* result is in better agreement with experiment. The number of atoms under the second peak in all the three  $g_2(r)$  are about 14. However, both Bellissent *et al.*<sup>1</sup> and Hafner<sup>8</sup> claimed that this number is about 9, considerably smaller than 14. From this inaccurate number, they concluded that the second peak in  $g_2(r)$  (the peak and the shoulder in the experimental result) corresponded to the second (three atoms) and third (six atoms) neighbor shells in the rhombohedral structure. It seems to us that this is not the case. The number of atoms un-

TABLE I. Properties of liquid arsenic in comparison with those of crystals. The *ab initio* simulations are performed with 64 atoms and  $E_{\text{cut}} = 12$  Ry; the pair-potential simulations are performed with 500 atoms,  $R_c = 5.7$  Å, and  $R_{\text{core}} = 0.53$  Å; experimental results are taken from Ref. 1 and properties of crystals are taken from Ref. 2.

Property	Crystal rhombohedral	Crystal orthorhombic	Liquid <i>ab initio</i>	Liquid pair potential	Liquid expt.
Coordination number	3	3	3	4	3
First peak (Å)	2.51	2.48/2.49	2.45 (2.50) <sup>a</sup>	2.61 (2.68) <sup>a</sup>	2.50
No. of atoms	3	3	3.82	4.48	3.9
Second peak (Å)	3.14, 3.76, 4.13	many	3.54, 4.10	3.85	3.4, 3.75 (4.1) <sup>b</sup>
No. of atoms	3+6+6	3+6+6	14.1	13.7	15.0
Bond angle	97.2°	94.1°/98.5°	80–125°	65–130°	
Pyramid height (Å)	1.25	1.25	~1.25		
Pyramid angle	180°	180°/48°	~180°		
Energy gap (eV)	0	0.3	0.15		0.5

<sup>a</sup>The number in parentheses is the peak position after broadening that should be compared with experiment.

<sup>b</sup>The peak at 4.1 Å is hardly visible.

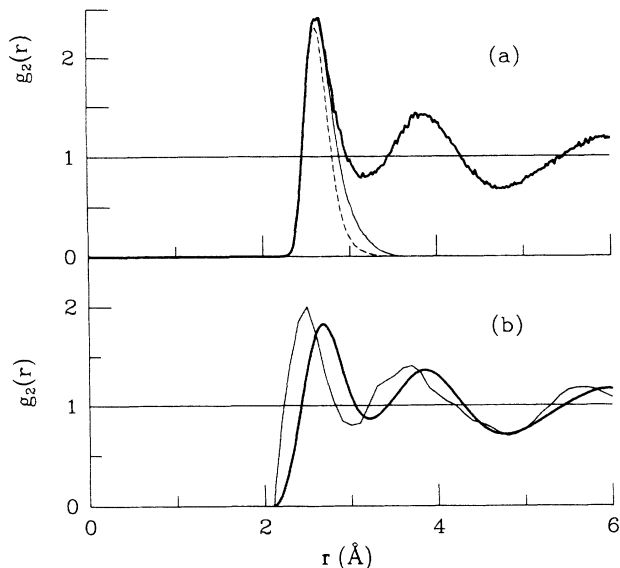


FIG. 15. (a) Analysis of the pair-correlation function at low density from pair-potential simulations. Thick line is the same as the thick line in Fig. 13; thin dashed and solid lines are the  $g_2(r)$  for three and four nearest-neighbor atoms, respectively. (b) Comparison with experiment. Thick line is the  $g_2(r)$  broadened with  $q_{\max} = 13 \text{ \AA}^{-1}$ ; thin line is the experimental result from Ref. 1.

der the first and second peaks add up to about 18 for all the three  $g_2(r)$ , evidently corresponding to the first four shells in the rhombohedral structure, or the first two shells in a simple-cubic structure.

The second peak in  $g_2(r)$  shows interesting differences among the three results. Experiment gave a major peak at 3.75 Å, a shoulder at 3.4 Å, and some feature hardly visible near 4.1 Å, in good coincidence to the peaks in rhombohedral structure 3.14, 3.76, and 4.13 Å. The *ab initio* simulations give two almost separate peaks at 3.54 and 4.10 Å. The 3.54 Å peak can be identified as the sum of the 3.14 and 3.76 Å peaks in the rhombohedral structure. The pair-potential simulations give a single peak at 3.83 Å without any evidence of coming from three peaks. Therefore, the results of the *ab initio* simulations are qualitatively more similar to those of the experiment than of the pair-potential simulations. It is unlikely that the Friedel oscillations could correctly reproduce the fine structures on the second peak of  $g_2(r)$ . The Peierls distortion and Friedel modulation pictures may not contradict each other, though the former is not perturbative and the latter is. If we have to choose one, then the Peierls distortion picture is preferable.

While the static structure factors  $S(q)$  and the bond-angle distribution functions  $g_3(\cos\theta)$  have no qualitative differences between the two simulations, the pyramid height distribution functions  $g_4(r)$  (Figs. 16 and 8) are very different. In the *ab initio* case,  $g_4(r)$  has a peak around 1.25 Å, whereas the pair-potential result shows more uniform behavior, implying that the shape of py-

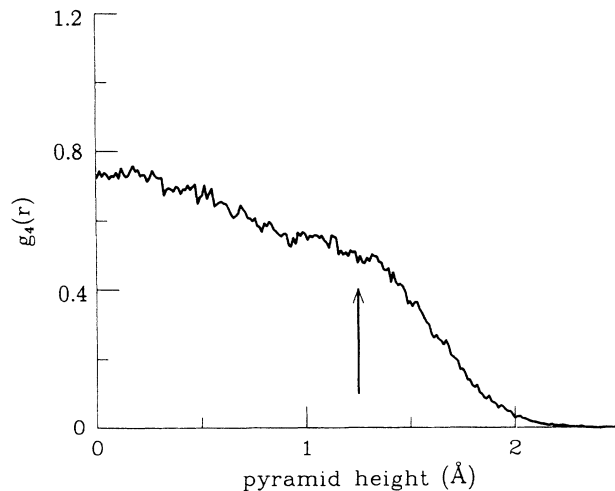


FIG. 16. Pyramid-height distribution function from pair-potential simulations for near the triple-point liquid arsenic. The arrow is the value of crystal structures.

ramids is random. This confirms that the local structure predicted by the pair potential is significantly different from the *ab initio* result. Pyramids are less well defined because the fourth neighbor is not expelled from the first shell of atoms. The *ab initio* predictions for the liquid bear a closer resemblance to crystalline structures of arsenic than do the pair-potential predictions.

The diffusion coefficient estimated from pair-potential simulations is about  $6.5 \times 10^{-5} \text{ cm}^2/\text{sec}$ , in good agreement with the *ab initio* estimation. Summarized comparison of properties from experiment, *ab initio* and pair-potential simulations are given in Table I.

## V. LIQUID ARSENIC AT HIGH DENSITY AND HIGH TEMPERATURE

The structural phase transformations of matter under various conditions are always an important issue in condensed matter physics, and the possible disappearance of the Peierls distortion makes it particularly interesting for liquid arsenic. In this section we investigate possible structural changes of liquid arsenic at high density and high temperature from both *ab initio* and pair-potential simulations.

### A. High density

In their linear augmented-plane-wave (LAPW) calculations, Mattheiss *et al.*<sup>6</sup> found a phase transformation of crystal arsenic from rhombohedral to simple-cubic structure at the volume of about  $17 \text{ \AA}^3/\text{atom}$  and under a pressure of about 190 kbar. In order to see if such a transformation also occurs in liquid arsenic, we perform simulations at the volume of  $15.88 \text{ \AA}^3/\text{atom}$ .

The conditions for the *ab initio* simulations are exactly the same as described in Sec. III except that the number of plane waves is less as a result of the smaller volume and a constant energy cutoff. Several pair-potential simu-

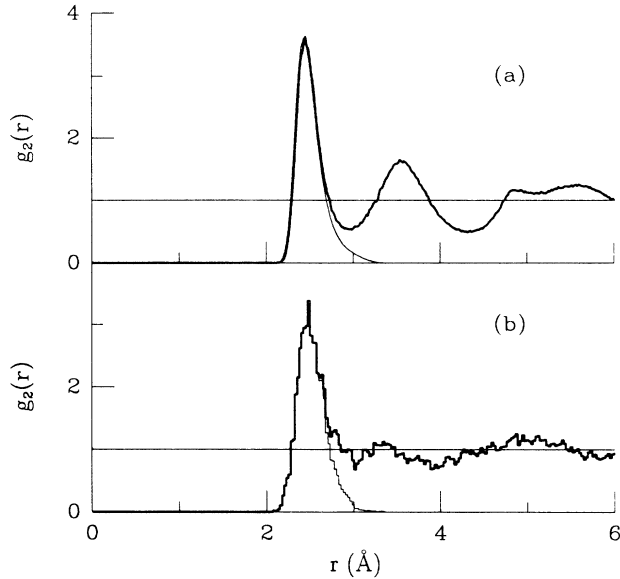


FIG. 17. Pair-correlation function  $g_2(r)$  for high-density liquid arsenic from pair-potential simulations (a) and from *ab initio* simulations (b). The thin lines are the pair-correlation functions for six nearest-neighbor atoms.

lations are carried out with different choices of core radius  $R_{\text{core}}$  in the empty core pseudopotential, and all the results are extremely similar except the height of the first peak in  $g_2(r)$ . Therefore, we describe here the results from a particular set of simulations using the pair potential shown in Fig. 3 by the thin solid line, which is generated with  $R_{\text{core}} = 0.53 \text{ \AA}$ , the same as Hafner's choice for his near the triple-point simulations, and again only the first oscillation of the potential is retained, and the number of atoms is 500.

The pair-correlation functions are shown in Fig. 17, and the pair-correlation functions for the six-nearest-neighbor atoms are also shown. From both simulations, the coordination number can be identified as 6, and the first peaks from the two simulations are very similar. However, as shown in Table II, the second peak in  $g_2(r)$  from the *ab initio* and pair-potential simulations are very different. The bond-angle distribution functions are even

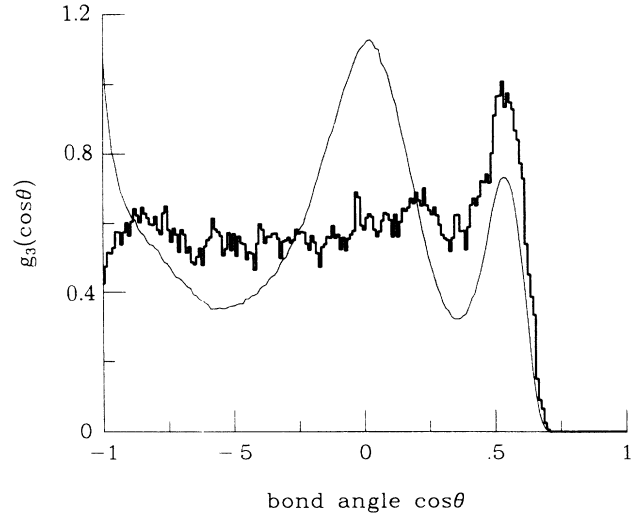


FIG. 18. Bond-angle distribution function  $g_3(\cos\theta)$  for high-density liquid arsenic from pair-potential simulations (thin line) and *ab initio* simulations (histogram).

more different, as shown in Fig. 18.

The results from the pair-potential simulations suggest an interpretation by a simple-cubic-like structure. In a simple-cubic crystal structure, the number of atoms under the first two peaks are 6 and 12, respectively, and the position of the second peak is  $\sqrt{2}$  times the position of the first peak. In the pair-potential result, the number of atoms under the first two peaks are 6.27 and 13.96, respectively, very close to 6 and 12. The first two peaks are centered at 2.45 and 3.50 Å, and  $\frac{3.50}{2.44} = 1.43 \approx \sqrt{2}$ . The similarity between the two structures is evident. This observation is strongly supported by the bond-angle distribution function, in which big peaks exist at  $\theta \sim 90^\circ$  and  $180^\circ$ , just as in a simple-cubic structure. The subsidiary maximum at  $\theta \sim 60^\circ$  has no simple explanation. It could be due to next nearest neighbors or some kind of defects.

The results from *ab initio* simulations are more difficult to explain. The number of atoms under the first two peaks in  $g_2(r)$  are 7.3 and 7.7, respectively, both close to 6, and the peak positions are 2.49 Å and 3.34 Å. A good

TABLE II. Properties of liquid arsenic at high density. The volume is  $15.88 \text{ \AA}^3/\text{atom}$ .

Property	<i>ab initio</i>	Pair potential
pressure	$\sim 60$ kbar	
coordination No.	6	6
1st peak position (Å)	2.49	2.45
No. of atoms	7.3	6.27
2nd peak position (Å)	3.34	3.50
No. of atoms	7.7	13.96
bond angle	$\sim 60^\circ$	$\sim 90^\circ, 180^\circ (60^\circ)$
similar crystal structure	simple rhombohedral	simple cubic
transformation	possibly first order	possibly smooth
electronic character	metal	metal
dc resistivity ( $\mu\Omega \text{ cm}$ )	$40 \pm 10$	$\sim 57$

candidate is a simple-rhombohedral-like structure, the difference between which and an  $A7$  structure is that in an  $A7$  structure, there are two atoms in a unit cell, but in a simple rhombohedral structure, there is only one atom in a unit cell. The simple rhombohedral structure has three qualitatively different types characterized by different angle  $\theta$  between two basis vectors: (1)  $\theta > 90^\circ$ , which can be viewed as a simple cubic flattened along the threefold axis; (2)  $60^\circ < \theta < 90^\circ$ , an elongated simple cubic or a flattened fcc along the threefold axis; and (3)  $\theta < 60^\circ$ , an elongated fcc along diagonal. From the  $g_2(r)$  shown in Fig. 17(b), we can exclude the possibility of (1) and (2), because otherwise the position of the third peak would be at about 3.7 Å, indistinguishable from the second peak. Therefore the high-density liquid arsenic generated from *ab initio* simulations has a simple-rhombohedral-like, or an elongated-fcc-like structure. From the position of the first two peaks, we estimate the position of the third peak to be at about 4.2 Å, beyond the second minimum in  $g_2(r)$  and  $\theta$  to be about  $44^\circ$ . Notice that this  $\theta$  is not the bond angle in this case. It is more clear to look at the structure along the threefold axis. In fcc structure, the interlayer distance is  $c = \sqrt{\frac{2}{3}}d \sim 0.82d$ , where  $d$  is the nearest-neighbor distance; whereas in liquid arsenic,  $c \approx 1.2d$  with  $d \approx 2.49$  Å. All the neighbors are within the layer and the bond angle is  $60^\circ$ , which is consistent with the bond angle distribution function. It is interesting to notice that all the above analysis will be equally valid if we assume a hexagonal structure instead of a simple-rhombohedral structure, and it would be nice to distinguish the two cases, which unfortunately requires the examination of the correlations between atoms about 6 Å apart, and at that range the result is no longer reliable because of the long-range disorder in a liquid, as well as the small size of the system. We leave this uncertainty as a subject for further studies. The area under the  $60^\circ$  peak in  $g_3(\cos\theta)$  is only a very small fraction of the whole area, indicating that the structure is less ordered.

Comparing the  $g_2(r)$  and  $g_3(\cos\theta)$  at high density described in this section and those at low density described in Secs. III and IV, we find that the *ab initio* results are very different, possibly implying a first-order phase change in between; but the pair-potential results are extremely similar except that the number of atoms under the first peak in  $g_2(r)$  increases from about 4.5 to about 6.3, indicating that the structure changes smoothly from low density to high density. The *ab initio* pseudopotential calculations of Needs *et al.*<sup>4</sup> suggested that the simple-cubic structure is always unstable against the rhombohedral structure, and at very high density the rhombohedral structure would transform directly to a close packed structure without going through a simple-cubic structure as an intermediate state. This result seems to be consistent with our *ab initio* simulations from which we find high-density liquid arsenic to be close to a close packed structure, although we do not know if a sc-like phase would exist at a density between our high and low densities.

All the three groups<sup>4-6</sup> that studied the structural properties of crystal arsenic predicted that at all volumes, the sc structure is stable against simple-rhombohedral

distortions. This is not contradictory to our finding for liquid arsenic, because the stable structure we find is type (3) defined earlier (the angle between two basis vectors is  $\theta < 60^\circ$ ), whereas they only checked types (1) and (2) with  $\theta$  close to  $90^\circ$ . Whether the liquid structure is still similar to the crystal structure at high density is another interesting subject for further studies, which can be qualitatively determined by examining the stability of the fcc structure against rhombohedral distortions.

The *ab initio* method used here does not have a pressure algorithm. To give a rough idea how large the pressure is, we use the calculated energies at the two volumes and the experimental triple-point pressure to estimate the pressure at high density from the following formula:<sup>43</sup>

$$E = a \left[ \frac{1}{V} - \frac{1}{V_0} \right]^2 + E_0, \quad (11)$$

and find the pressure of the high-density liquid arsenic to be about 60 kbar. This number is not accurate, but it suggests that if the phase transformation indeed exists, it should be easily observable by experiment.

The electronic DOS, the participation ratio and the imaginary part of the dielectric constant from the *ab initio* simulations are shown in Figs. 19–21. The  $s$  states and  $p$  states are no longer separated from each other and the participation ratio remains roughly a constant throughout the spectrum. There is still no evidence of electronic localization. Although the DOS still has a minimum at the Fermi energy, liquid arsenic is clearly a metal, as also shown by the behavior of  $\epsilon_2(\omega)$ , which seems to diverge as  $\omega$  tends to 0, consistent with the experimental result of Alekseev *et al.*,<sup>44</sup> where the conductivity of liquid arsenic at 330 atm (much lower than our pressure) was measured and showed metallic behavior (already). Although the electronic DOS of liquid arsenic from pair potential has not been calculated, it can be guessed from the calculation of Mattheiss *et al.*<sup>6</sup> since it

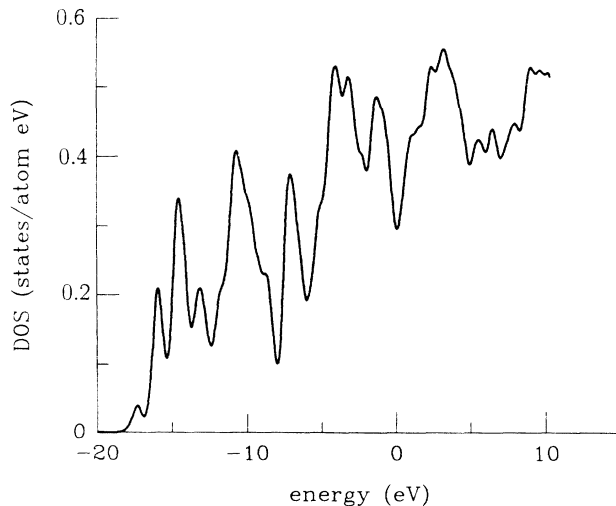


FIG. 19. Electronic DOS for high-density liquid arsenic from *ab initio* simulations.

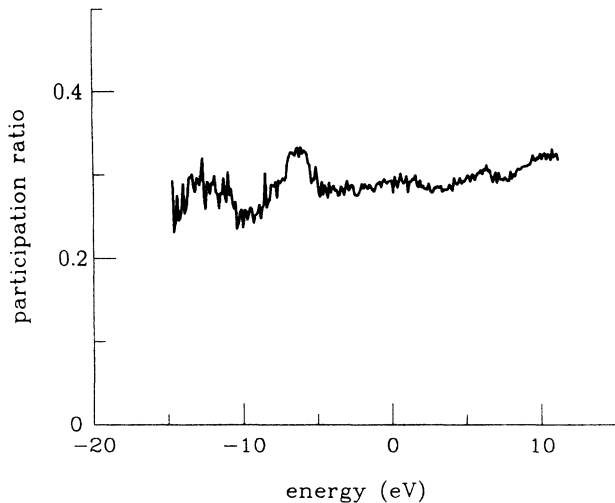


FIG. 20. Participation ratio of electronic state for high-density liquid arsenic from *ab initio* simulations.

has a simple-cubic-like structure. High-density liquid arsenic generated from pair-potential simulations is then also probably a metal.

Figure 22 shows the electrical conductivity as a function of frequency for liquid arsenic from *ab initio* simulations. At  $\omega \sim 0$ , the statistics are bad, which is reflected by the large scattering of the data at that range. The thin lines show two possible fittings of  $\sigma(\omega)$  to the Drude formula

$$\sigma(\omega) = \frac{\omega_p^2 / \tau}{4\pi(\omega^2 + 1/\tau^2)}, \quad (12)$$

showing that  $\sigma(\omega)$  is Drude-like at large  $\omega$ , but deviates significantly from Drude behavior at small  $\omega$ . The dc resistivity is  $40 \pm 10 \mu\Omega \text{ cm}$ .

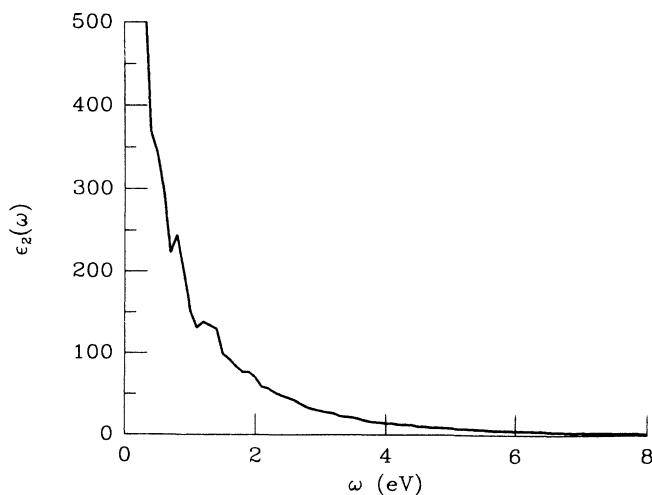


FIG. 21. Imaginary part of the dielectric constant for high-density liquid arsenic from *ab initio* simulations.

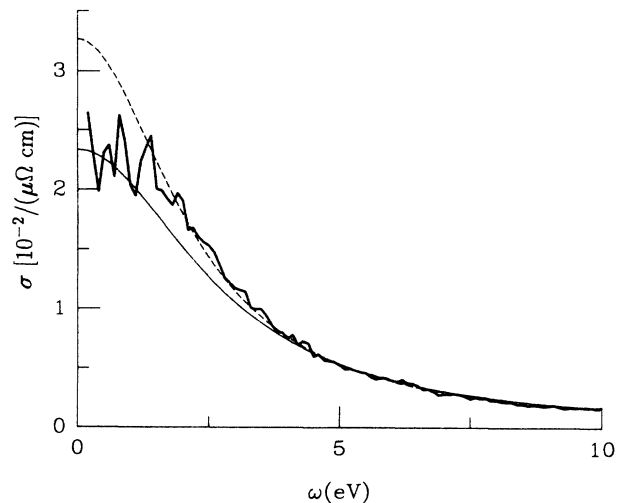


FIG. 22. Electrical conductivity for high-density liquid arsenic from *ab initio* simulations (thick line) and two fittings to the Drude formula (thin lines).

The dc resistivity of liquid arsenic from the pair-potential simulations can be calculated using Ziman formula<sup>45</sup>

$$\rho = \frac{3\pi m^2 \Omega}{4\hbar^3 e^2 k_F^6} \int_0^{2k_F} S(q) [U(q)]^2 q^3 dq, \quad (13)$$

where  $U(q)$  is the screened pseudopotential of a single ion,  $S(q)$  the structure factor of the liquid that is a result of our pair-potential simulations, and  $k_F$  the wave number of the electrons at Fermi surface. We find  $\rho \simeq 57 \mu\Omega \text{ cm}$ , marginally within the error bar of the *ab initio* result.

## B. High temperature

The possible structural changes of liquid arsenic at very high temperature ( $\sim 2450 \text{ K}$ ) are also investigated by means of both pair-potential and *ab initio* simulations. The pair-correlation functions and bond-angle distribution functions are similar to the near triple-point results except some minor differences that may be explained by the temperature effect. Therefore, no structural transformation is observed. Recently, Bergman *et al.*<sup>46</sup> reported the pair-correlation function of liquid arsenic at about  $1400 \text{ K}$  from neutron-scattering experiment. They found that the structure is almost not changed. This seems true from our calculations up to the temperature of  $2450 \text{ K}$ .

## VI. SUMMARY AND CONCLUSIONS

The present work contains the most detailed comparison of local structure in a liquid as derived by two different methods: *ab initio* LDA versus a perturbative pair potential. The degree of success of pair potentials is surprising and impressive—the pair-correlation functions and the bond-angle distribution functions agree fair-

ly well with the *ab initio* results, and the high-density crossover to a new structure comes out reasonably with a correct coordination number. But the fine details are not quite right—in the near triple point structure, the fourth atom is not successfully expelled from the first shell of atoms, and as a result the pyramids are less well defined; the high-density liquid structure is different from the *ab initio* result, and the nature of the crossover is probably different. From both calculations, the pair-correlation functions are in reasonable agreement with experiment.

A transformation should occur in liquid arsenic from a threefold coordinated semiconductor to a sixfold coordinated metal when pressure is increased but not when temperature is increased. The volume at the crossover should be  $\geq 16 \text{ \AA}^3/\text{atom}$ , and the pressure is accessible by experiment. The *ab initio* simulations show that the near triple-point liquid has a very similar structure to the *A7* crystal, and the new phase at high density is similar to a rhombohedral or a hexagonal structure close to a close-packed structure, with 6 nearest neighbors, and the

crossover is probably first order. We hope our theoretical findings can stimulate some experimental work.

#### ACKNOWLEDGMENTS

The author thanks P. B. Allen, J. Q. Broughton, R. Car, and M. Parrinello for constant encouragement and helpful advice and for providing computer programs; G. L. Chiarotti and X. Ren for help with computer programs; and D. C. Allan, J. D. Althoff, J. W. Davenport, G. W. Fernando, J. Hafner, J. D. Joannopoulos, G.-X. Qian, and M. T. A. Weinert for useful discussions. This work is partially supported by the National Science Foundation (NSF) under Grant No. DMR-88-14311 and the U.S. Department of Energy (Division of Materials Science of the Office of Basic Energy Sciences) under Contract No. DE-AC02-76CH00016. Most of the calculations were done on the Cray Research, Inc. X-MP supercomputer at Pittsburgh Supercomputer Center, with support from NSF.

\*Present address: Department of Physics, University of Illinois at Urbana-Champaign, 1110 West Green Street, Urbana, IL 61801.

<sup>1</sup>R. Bellissent, C. Bergman, R. Ceolin, and J. P. Gaspard, *Phys. Rev. Lett.* **59**, 661 (1987).

<sup>2</sup>G. N. Greaves, S. R. Elliot, and E. A. Davis, *Adv. Phys.* **28**, 49 (1979).

<sup>3</sup>P. Hohenberg and W. Kohn, *Phys. Rev.* **136**, B864 (1964); W. Kohn and L. J. Sham, *Phys. Rev.* **140**, A1133 (1965).

<sup>4</sup>R. J. Needs, R. M. Martin, and O. H. Nielsen, *Phys. Rev. B* **33**, 3778 (1986); **35**, 9851 (1987).

<sup>5</sup>K. J. Chang and M. L. Cohen, *Phys. Rev. B* **33**, 7371 (1986).

<sup>6</sup>L. F. Mattheiss, D. R. Hamann, and W. Weber, *Phys. Rev. B* **34**, 2190 (1986).

<sup>7</sup>J. P. Gaspard, F. Parrinello, and A. Pellegatti, *Europhys. Lett.* **3**, 1095 (1987).

<sup>8</sup>J. Hafner, *Phys. Rev. Lett.* **62**, 784 (1989).

<sup>9</sup>W. Jank and J. Hafner, *Europhys. Lett.* **7**, 632 (1988).

<sup>10</sup>Y. Abe, I. Ohkoshi, and A. Morita, *J. Phys. Soc. Jpn.* **42**, 504 (1977); A. Morita, I. Ohkoshi, and Y. Abe, *ibid.* **43**, 1610 (1977).

<sup>11</sup>I. V. Berman and N. B. Brandt, *Pis'ma Zh. Eksp. Teor. Fiz.* **10**, 88 (1969) [*JETP Lett.* **10**, 55 (1969)]; M. J. Duggin, *J. Phys. Chem. Solids* **33**, 1267 (1972); H. Kawamura and J. Wittig, *Physica B+C (Amsterdam)* **135B**, 239 (1985).

<sup>12</sup>D. R. Hamann, M. Schlüter, and C. Chiang, *Phys. Rev. Lett.* **43**, 1444 (1979); G. B. Bachelet, D. R. Hamann, and M. Schlüter, *Phys. Rev. B* **26**, 4199 (1982).

<sup>13</sup>X.-P. Li, P. B. Allen, R. Car, M. Parrinello, and J. Q. Broughton, *Phys. Rev. B* **41**, 3260 (1990).

<sup>14</sup>R. Car and M. Parrinello, *Phys. Rev. Lett.* **55**, 2471 (1985).

<sup>15</sup>D. Hohl, R. O. Jones, R. Car, and M. Parrinello, *Chem. Phys. Lett.* **139**, 540 (1987).

<sup>16</sup>R. Car and M. Parrinello, *Phys. Rev. Lett.* **60**, 204 (1988).

<sup>17</sup>P. Ballone, W. Andreoni, R. Car, and M. Parrinello, *Phys. Rev. Lett.* **60**, 271 (1988).

<sup>18</sup>G. Galli, R. Martin, R. Car, and M. Parrinello, *Phys. Rev. Lett.* **62**, 555 (1989).

<sup>19</sup>R. Car (private communication).

<sup>20</sup>G. W. Fernando, G.-X. Qian, M. Weinert, and J. W. Davenport, *Phys. Rev. B* **40**, 7985 (1989).

<sup>21</sup>I. Štich, R. Car, and M. Parrinello, *Phys. Rev. Lett.* **63**, 2240 (1989).

<sup>22</sup>Q.-M. Zhang, G. Chiarotti, A. Selloni, R. Car, and M. Parrinello (unpublished).

<sup>23</sup>G. Galli, R. Martin, R. Car, and M. Parrinello, *Phys. Rev. Lett.* **63**, 988 (1989).

<sup>24</sup>G.-X. Qian, G. W. Fernando, M. Weinert, and J. W. Davenport (unpublished).

<sup>25</sup>J. Q. Broughton and X.-P. Li, *Phys. Rev. B* **35**, 9120 (1987); X.-P. Li, G. Chen, P. B. Allen, and J. Q. Broughton, *ibid.* **38**, 3331 (1988).

<sup>26</sup>V. Heine and D. Weaire, in *Solid State Physics*, edited by H. Ehrenreich, F. Seitz, and D. Turnbull (Academic, New York, 1970), Vol. 24, p. 249; N. W. Ashcroft and D. Stroud, in *Solid State Physics*, edited by H. Ehrenreich, F. Seitz, and D. Turnbull (Academic, New York, 1978), Vol. 33, p. 1.

<sup>27</sup>J. Hafner and V. Heine, *J. Phys. F* **13**, 2479 (1983).

<sup>28</sup>J. Hafner and G. Hahl, *J. Phys. F* **14**, 2259 (1984).

<sup>29</sup>S. Ichimaru and K. Utsumi, *Phys. Rev. B* **24**, 7385 (1981).

<sup>30</sup>N. W. Ashcroft, *Phys. Lett.* **23**, 48 (1966).

<sup>31</sup>L. Kleinman and D. M. Bylander, *Phys. Rev. Lett.* **48**, 1425 (1982); D. C. Allan and M. P. Teter, *ibid.* **59**, 1136 (1987).

<sup>32</sup>R. Bellissent (private communication).

<sup>33</sup>W. Klemm, H. Spitzer, and H. Niermann, *Angew. Chem.* **72**, 985 (1960).

<sup>34</sup>P. J. McGonigal and A. V. Grosse, *J. Phys. Chem.* **67**, 924 (1963).

<sup>35</sup>X.-P. Li, P. B. Allen, R. Car, and M. Parrinello, in *Proceedings of the Materials Research Society Symposium*, edited by J. Tersoff, D. Vanderbilt, and V. Vitek (MRS, Boston, 1988), Vol. 141, p. 229.

<sup>36</sup>A. Rahman and F. H. Stillinger, *J. Chem. Phys.* **55**, 3336 (1971).

<sup>37</sup>G. Etherington, A. C. Wright, J. T. Wenzel, J. C. Dore, J. H. Clarke, and R. N. Sinclair, *J. Non-Cryst. Solids* **48**, 265 (1982).

<sup>38</sup>E. N. Economou, *Green's Functions in Quantum Physics*, Vol.

- 7 of *Solid State Sciences*, edited by P. Fulde (Springer, Berlin, 1983).
- <sup>39</sup>P. B. Allen and J. Q. Broughton, *J. Phys. Chem.* **91**, 4964 (1987).
- <sup>40</sup>P. B. Allen and J. L. Feldman, *Phys. Rev. Lett.* **62**, 645 (1989).
- <sup>41</sup>M. S. Hybertsen and S. G. Louie, *Phys. Rev. B* **35**, 5585 (1987).
- <sup>42</sup>S. Baroni and R. Resta, *Phys. Rev. B* **33**, 7017 (1986).
- <sup>43</sup>P. K. Lam and M. L. Cohen, *Phys. Rev. B* **24**, 4224 (1981).
- <sup>44</sup>V. A. Alekseev, V. G. Ovcharenko, Ju. F. Ryzhkov, and M. V. Sadovsky, *Phys. Lett.* **65A**, 173 (1978).
- <sup>45</sup>T. E. Faber, *An Introduction to the Theory of Liquid Metals* (Cambridge University Press, Cambridge, 1972), p. 67.
- <sup>46</sup>C. Bergman, A. Pellegatti, R. Bellissent, A. Menelle, R. Ceolin, and J. P. Gaspard, *Physica B (Amsterdam)* **156&157**, 158 (1989).